Renormalization-group-improved action on anisotropic lattices

S. Ejiri,[1] K. Kanaya,[2] Y. Namekawa,[2] and T. Umeda[3]
[1]*Department of Physics, University of Wales Swansea, Singleton Park, Swansea, SA2 8PP, United Kindom*
[2]*Institute of Physics, University of Tsukuba, Tsukuba, Ibaraki 305-8571, Japan*
[3]*Center for Computational Physics, University of Tsukuba, Tsukuba, Ibaraki 305-8577, Japan*
(Received 30 January 2003; published 8 July 2003)

We study a block spin transformation in the SU(3) lattice gauge theory on anisotropic lattices to obtain Iwasaki's renormalization-group-improved action for anisotropic cases. For the class of actions with plaquette and 1×2 rectangular terms, we determine the improvement parameters as functions of the anisotropy $\xi = a_s/a_t$. We find that the program of improvement works well also on anisotropic lattices. From a study of an indicator which estimates the distance to the renormalized trajectory, we show that, for the range of the anisotropy $\xi\approx1-4$, the coupling parameters previously determined for isotropic lattices improve the theory considerably.

DOI: 10.1103/PhysRevD.68.014502 PACS number(s): 11.15.Ha, 12.38.Gc

I. INTRODUCTION

Improvement and anisotropy are two key ingredients of the recent developments in lattice QCD. In QCD with dynamical quarks, the improvement of the lattice theory is essential to perform a continuum extrapolation of light hadron spectra within the computer power currently available [1,2]. At finite temperatures, the expected O(4) scaling around the two-flavor chiral transition point is reproduced on the lattice only with improved Wilson-type quarks [3,4]. Improved actions are applied also for staggered-type quarks to reduce lattice artifacts [5,6]. However, in order to perform a continuum extrapolation of thermodynamic quantities, we need to further increase the temporal lattice size N_t [7,8]. This requires quite large spatial lattice sizes to keep the system close to the thermodynamic limit, and the task slightly exceeds the current limit of the computer power for QCD with dynamical quarks [9].

Recently, we proposed to apply anisotropic lattices for reducing the computational demand in thermal QCD [10]. Because the dominant part of the lattice artifacts in the equation of state (EOS) is due to the finite temporal cutoff, an anisotropic lattice with a larger temporal cutoff will provide us with an efficient way to calculate thermodynamic quantities. We tested the idea for the case of the SU(3) gauge theory with the standard one-plaquette action. From a series of simulations at $N_t/\xi=4$, 5, and 6 with anisotropy $\xi \equiv a_s/a_t=2$, where a_s and a_t are the spatial and temporal lattice spacings, we find that the lattice artifacts in the EOS are much smaller than those on the corresponding isotropic lattice, and the leading scaling relation is satisfied from the coarsest lattice. This enabled us to perform a well-controlled continuum extrapolation of the EOS in QCD. Anisotropic lattices have been employed also to study transport coefficients and temporal correlation functions in finite temperature QCD [11–13]. In these studies, anisotropy was introduced to obtain more data points for temporal correlation functions. At zero temperature, anisotropic lattices have been employed to study charmonium states [14–16], heavy hybrids [17], glueballs [18], and also the pion scattering length [19].

A combination of the ideas of improvement and anisotropy is not straightforward, however. The main difficulty is the large number of coupling parameters in improved actions on anisotropic lattices. Even in the simplest case of the renormalization-group- (RG-) improved gauge action by Iwasaki [20], which contains plaquette and 1×2 rectangular terms only, we have five parameters on anisotropic lattices, instead of two for the isotropic case. We have to fix them as functions of two parameters: the gauge coupling β which controls the overall scale and the anisotropy ξ. Because the redundant parameters have no physical effects in the continuum limit, they have to be determined through a requirement of improvement—i.e., minimizing lattice artifacts in physical observables away from the continuum limit.

A concrete form of the dependence on the scale and anisotropy in the coupling parameters is important for a calculation of thermodynamic quantities [21–25]. In a Symanzik-type improvement program, it is easy to see that, at the tree level of perturbation theory, the coupling parameters are independent of ξ. Accordingly, studies of finite temperature Symanzik-type improved actions on anisotropic lattices have been done assuming isotropic improvement parameters [26–28]. When we improve the theory beyond the tree level, we have to take into account the ξ dependences in the coupling parameters. Isotropic parameters have been adopted also in a study of the RG-improved action on anisotropic lattices [11], however, without justifying the choice.

In this paper, we study the anisotropic improvement parameters for the RG improved gauge action. Following Iwasaki's program of RG improvement using a block spin transformation, we determine the values of coupling parameters which minimize the lattice discretization errors. After a brief explanation of the RG-improved action in Sec. II, the anisotropic gauge action we study is defined in Sec. III. We then study Wilson loops under a block spin transformation in Sec. IV. In Sec. V, RG-improved actions on anisotropic lattices are determined and a practical choice of the improved action for numerical simulations is discussed. We conclude in Sec. VI.

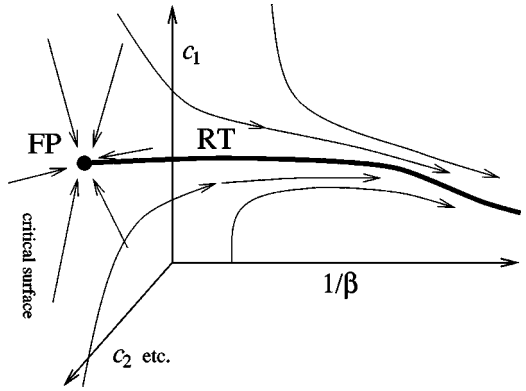

FIG. 1. RG flow and the renormalized trajectory for the SU(3) gauge theory in infinite dimensional coupling parameter space.

II. PROGRAM FOR RG-IMPROVED ACTION

Various lattice actions are expected to belong to a common universality class having the same continuum limit. For the SU(3) gauge theory, a lattice action may contain, for example, 1×2 rectangular loops, 2×2 squares, etc., in addition to the conventional plaquettes. One combination $\beta=2N_c/g^2$ of the coupling parameters is the relevant parameter which reflects the freedom of the lattice spacing, while other coupling parameters are redundant in the continuum limit. The objective of improvement is to find the values of redundant parameters for which physical observables from a coarse lattice are closest to their continuum values.

In order to discuss the improvement of a lattice action, we consider RG flows of a block spin transformation as shown in Fig. 1. The block spin transformation halves the correlation length in lattice units but does not change the long-range properties of the system. Then, the coupling parameter moves toward smaller β corresponding to the correlation length becoming shorter. In this figure, c_1, c_2, etc., denote the redundant coupling parameters, and the points on the $1/\beta$ axis correspond to the standard one-plaquette actions. The hyperplane at $\beta=\infty$ $(g=0)$, on which the correlation length diverges and the continuum limit can be taken, is called the critical surface. In this surface, the coupling parameter does not go out of the surface of $\beta=\infty$ under the block spin transformation, since the correlation length after the block spin transformation is also infinity, which means that an RG flow around $\beta=\infty$ runs parallel to the critical surface, except in the vicinity of a fixed point (FP), at which a coupling parameter does not change under the block spin transformation. Therefore, an RG flow can connect only at FP to the critical surface.

Moreover, because RG flows can be regarded as lines of constant physics, the distance between each RG flow becomes wider as β increases corresponding to physical quantities becoming more insensitive to the redundant coupling parameters, c_1, c_2, etc., as the continuum limit is approached, and only one RG flow which has properties in the continuum limit, called the renormalized trajectory (RT), can connect to the critical surface at FP by infinite block spin transformations.

The actions on the RT are ''perfect actions'' which reproduce continuum properties from the shortest distances on the lattice [29]. If an infinite number of coupling parameters are admitted, a perfect action is a goal of improvement. In reality, we are forced to keep the interactions as simple as possible in numerical simulations. Hence to find the nearest point to RT in the restricted coupling parameter space is the problem in practice. Iwasaki applied the program of improvement to the SU(N_c) gauge theory in the weak coupling limit for the case of the action with plaquette and 1×2 rectangular terms [20]. He found the nearest point to the fixed point in the coupling parameter subspace by calculating Wilson loops perturbatively on the lattice consisting of blocked link valuables after block spin transformations. Another approach of an RG-improved action is the classical perfect action approach in [29], which is suitable for increasing the coupling parameters. See [30] for a trial to include quantum corrections. A classically perfect action on anisotropic lattices was studied in [31].

III. GAUGE THEORY ON ANISOTROPIC LATTICE

On isotropic lattices, the RG-improved gauge action by Iwasaki [20], which consists of plaquettes $W^{(1\times1)}$ and 1×2 rectangular loops $W^{(1\times2)}$, is defined by

$$S_{imp}=-\beta\left\{\sum_{x,\mu>\nu}c_0W^{(1\times1)}_{\mu\nu}(x)+\sum_{x,\mu\neq\nu}c_1W^{(1\times2)}_{\mu\nu}(x)\right\}, \tag{1}$$

where $c_0+8c_1=1$ for normalization and $c_1=-0.331$ (-0.293) to optimize the action after one (two) block spin transformation(s) (see below for details). This action has been shown to lead to better rotation symmetry of heavy quark potential than the standard one plaquette action [2,32] and to suppress lattice artifacts associated with Wilson-type quarks at finite temperature [3]. This action was also reported to be efficient in suppressing chiral violations in domain-wall quarks [33]. In two-flavor full QCD with clover-improved Wilson quarks, the first systematic studies of the light hadron spectrum [1] and the finite temperature equation of state with Wilson-type quarks [4,8] have been carried out.

The generalization of Iwasaki's action to an anisotropic lattice is given by

$$\begin{aligned}S=&-\beta_s\left\{\sum_{x,i>j}c_0^sW^{(1\times1)}_{ij}(x)+\sum_{x,i\neq j}c_1^sW^{(1\times2)}_{ij}(x)\right\}\\&-\beta_t\left\{\sum_{x,k}c_0^tW^{(1\times1)}_{k4}(x)+\sum_{x,k}[c_1^tW^{(2\times1)}_{k4}(x)\right.\\&\left.+c_2^tW^{(1\times2)}_{k4}(x)]\right\},\end{aligned} \tag{2}$$

where we set $c_0^s+8c_1^s=1$ and $c_0^t+4c_1^t+4c_2^t=1$ for normalization. This form of the tree-level Symanzik-improved ac-

tion with mean field improvement was studied in [26–28]. Here, we study the RG transformation of this action to obtain an RG-improved action.[1]

Let us denote the lattice spacing in the μ direction as a_μ and the lattice size as N_μ. We consider the case $a_1=a_2=a_3\equiv a_s$, $a_4\equiv a_t$ and $N_1=N_2=N_3\equiv N_s$, $N_4\equiv N_t$ with sufficiently large N_s and N_t. Identifying the gauge field by $U_\mu(x)=\exp[iga_\mu A_\mu(x)]$, the conventional gauge action is recovered in the classical continuum limit when

$$\beta_s=\frac{2N_c}{g^2\xi},\quad \beta_t=\frac{2N_c\xi}{g^2}, \tag{3}$$

where $\xi=a_s/a_t$.

We perform the Fourier transformation of $A_\mu(x)$ by

$$A_\mu(x)=\int_k e^{ikx+ik_\mu a_\mu/2}\tilde{A}_\mu(k), \tag{4}$$

where $\int_k\equiv(1/\sqrt{N_s^3N_t})\Pi_{\mu=1}^4\Sigma_{k_\mu}$, $k_\mu=2\pi j_\mu/N_\mu a_\mu$, and j_μ is integer. Then, the action reads

$$S=\frac{1}{2}a_s^3a_t\prod_{\mu=1}^4\sum_{k_\mu}\left\{\sum_{i<j,a}\{1-c_1^s a_s^2(\hat{k}_i^2+\hat{k}_j^2)\}\tilde{f}_{ij}^a(k)\tilde{f}_{ij}^a(-k)+\sum_{i,a}(1-c_1^t a_s^2\hat{k}_i^2-c_2^t a_t^2\hat{k}_4^2)\tilde{f}_{i4}^a(k)\tilde{f}_{i4}^a(-k)\right\}+O[\tilde{A}^3], \tag{5}$$

with $\hat{k}_\mu=(2/a_\mu)\sin(k_\mu a_\mu/2)$ and $\tilde{f}_{\mu\nu}(k)=i[\hat{k}_\mu\tilde{A}_\nu(k)-\hat{k}_\nu\tilde{A}_\mu(k)]$. We adopt the lattice Lorentz gauge by adding the gauge fixing term:

$$S_{\rm gf}=a_s^3a_t\sum_x\ {\rm tr}\left[\sum_\mu\ \Delta_\mu A_\mu(x)\right]^2, \tag{6}$$

$$\Delta_\mu f(x)=\{f(x)-U_\mu^\dagger f(x-a_\mu\hat{\mu})U_\mu(x-a_\mu\hat{\mu})\}/a_\mu. \tag{7}$$

In order to simplify the notation, we redefine lattice momenta and the gauge field absorbing the lattice spacings as $k_\mu a_\mu\to k_\mu$, $\hat{k}_\mu a_\mu\to\hat{k}_\mu$, and $\tilde{A}_\mu a_\mu\to\tilde{A}_\mu$, in the following. Then, the lattice propagator, $\langle\tilde{A}_\mu^a(k)\tilde{A}_\nu^b(k')\rangle=\delta_{a,b}\delta(k+k')D_{\mu\nu}(k)$, is given by

$$D_{ij}^{-1}(k)=\sum_{l=1}^3\frac{1}{\xi}q_{li}(k)\hat{k}_l^2\delta_{ij}+\xi q_{4i}(k)\hat{k}_4^2\delta_{ij}-\frac{1}{\xi}(q_{ij}(k)-1)\hat{k}_i\hat{k}_j,$$

$$D_{i4}^{-1}(k)=-\xi(q_{i4}(k)-1)\hat{k}_i\hat{k}_4,$$

$$D_{4i}^{-1}(k)=-\xi(q_{4i}(k)-1)\hat{k}_4\hat{k}_i,$$

$$D_{44}^{-1}(k)=\sum_{l=1}^3\xi q_{l4}(k)\hat{k}_l^2+\xi^3\hat{k}_4^2, \tag{8}$$

where

$$q_{ij}(k)=1-c_1^s(\hat{k}_i^2+\hat{k}_j^2)\quad \text{for } i\neq j(=1,2,3),$$

$$q_{i4}(k)=q_{4i}(k)=1-c_1^t\hat{k}_i^2-c_2^t\hat{k}_4^2, \tag{9}$$

with $q_{\mu\mu}(k)=0$.

We consider the following Wilson loops:

$$W_{\mu\nu}(1\times1)=(1/N_c){\rm tr}[U_\mu(x)U_\nu(x+\hat{\mu})\times U_\mu^\dagger(x+\hat{\nu})U_\nu^\dagger(x)], \tag{10}$$

$$W_{\mu\nu}(2\times1)=(1/N_c){\rm tr}[U_\mu(x)U_\mu(x+\hat{\mu})U_\nu(x+2\hat{\mu})\times U_\mu^\dagger(x+\hat{\mu}+\hat{\nu})U_\mu^\dagger(x+\hat{\nu})U_\nu^\dagger(x)], \tag{11}$$

$$W_{\mu\nu\rho}({\rm chair})=(1/N_c){\rm tr}[U_\mu(x)U_\nu(x+\hat{\mu})U_\rho(x+\hat{\mu}+\hat{\nu})\times U_\mu^\dagger(x+\hat{\nu}+\hat{\rho})U_\rho^\dagger(x+\hat{\nu})U_\nu^\dagger(x)], \tag{12}$$

$$W_{\mu\nu\rho}(3\ {\rm dim})=(1/N_c){\rm tr}[U_\mu(x)U_\nu(x+\hat{\mu})U_\rho(x+\hat{\mu}+\hat{\nu})\times U_\mu^\dagger(x+\hat{\nu}+\hat{\rho})U_\nu^\dagger(x+\hat{\rho})U_\rho^\dagger(x)]. \tag{13}$$

To the leading order of perturbation theory, we get [20,35]

$$\langle W(C)\rangle\equiv1-g^2\frac{N_c^2-1}{4N_c}F(C), \tag{14}$$

$$F_{\mu\nu}(I\times J)=(N_s^3N_t)^{-1}\prod_{\rho=1}^4\sum_{k_\rho}\left(\frac{\sin(Ik_\mu/2)}{\sin(k_\mu/2)}\frac{\sin(Jk_\nu/2)}{\sin(k_\nu/2)}\right)^2\times D_{\mu\nu,\mu\nu}(k), \tag{15}$$

$$F_{\mu\nu\rho}({\rm chair})=(N_s^3N_t)^{-1}\prod_{\sigma=1}^4\sum_{k_\sigma}\left[D_{\mu\nu,\mu\nu}(k)+D_{\mu\rho,\mu\rho}(k)-\frac{1}{2}[\hat{k}_\mu^2\hat{k}_\nu\hat{k}_\rho D_{\nu\rho}(k)+\hat{k}_\nu^2\hat{k}_\rho^2D_{\mu\mu}(k)-\hat{k}_\mu\hat{k}_\nu^2\hat{k}_\rho D_{\mu\rho}(k)-\hat{k}_\mu\hat{k}_\nu\hat{k}_\rho^2D_{\mu\nu}(k)]\right], \tag{16}$$

[1]Because our action contains couplings extending over two time slices, unphysical higher-lying states may contaminate correlation functions at short distances comparable to the extent of the action, as observed, e.g., in a study of glueball spectrum using a Symanzik improved gauge action [34]. Although these unphysical states do not affect physical properties at long distances, caution is required when we have to study short distance correlators to extract physical quantities.

$$F_{\mu\nu\rho}(3\ \mathrm{dim}) = (N_s^3 N_t)^{-1} \prod_{\sigma=1}^{4} \sum_{k_\sigma} [(1-\hat{k}_\rho^2/4) D_{\mu\nu,\mu\nu}(k) + (1-\hat{k}_\mu^2/4) D_{\nu\rho,\nu\rho}(k) + (1-\hat{k}_\nu^2/4) D_{\rho\mu,\rho\mu}(k)], \tag{17}$$

for $SU(N_c)$ gauge theory, where $D_{\mu\nu,\mu\nu}(k) = \hat{k}_\mu^2 D_{\nu\nu}(k) - \hat{k}_\mu \hat{k}_\nu D_{\nu\mu}(k) - \hat{k}_\nu \hat{k}_\mu D_{\mu\nu}(k) + \hat{k}_\nu^2 D_{\mu\mu}(k)$.

IV. BLOCK SPIN TRANSFORMATION

The purpose of this study is to find a fixed point at which the parameters in the action do not change. As seen in the previous section, $F(C)$ are functions of the redundant parameters $c_i^{s/t}$; hence, if a block spin transformation is performed in the vicinity of the fixed point, the values of $F(C)$ should not change. In this section, we calculate Wilson loops on the blocked lattice after block spin transformations in the $g \to 0$ limit and discuss the fixed point.

Following Iwasaki [20], we consider a simple block spin transformation from N_{BS}th to $(N_{\mathrm{BS}}+1)$th blocking of the form

$$A_\mu^{(N_{\mathrm{BS}}+1)}(n') = \frac{1}{8} \sum_{n \in n'} A_\mu^{(N_{\mathrm{BS}})}(n), \tag{18}$$

where we block 2^4 links at the sites $n = 2n' + \Sigma_\mu \epsilon_\mu \hat{\mu}$, ($\epsilon_\mu = 0,1$) to 1 link at n' on the blocked lattice. The lattice spacings change from a_μ to $2a_\mu$ by this transformation, while the anisotropy remains the same. Note that the scale factor 2 is multiplied on the right-hand side of Eq. (18) to scale back to the original lattice spacings, so that the relevant coupling g remains constant.

Link variables on the blocked lattice are defined by $U_\mu^{(N_{\mathrm{BS}})}(n) = \exp[iga_\mu A_\mu^{(N_{\mathrm{BS}})}(n)]$. Wilson loops consisting of blocked links are given by [20]

$$\langle W^{(N_{\mathrm{BS}})}(C) \rangle \equiv 1 - g^2 \frac{N_c^2 - 1}{4N_c} F^{(N_{\mathrm{BS}})}(C), \tag{19}$$

$$F_{\mu\nu}^{(N_{\mathrm{BS}})}(I \times J) = (N_s^3 N_t)^{-1} \times \prod_{\rho=1}^{4} \sum_{k_\rho} \left(\frac{\sin(Ik_\mu^{(N_{\mathrm{BS}})}/2)}{\sin(k_\mu^{(N_{\mathrm{BS}})}/2)} \frac{\sin(Jk_\nu^{(N_{\mathrm{BS}})}/2)}{\sin(k_\nu^{(N_{\mathrm{BS}})}/2)} \right)^2 \times D_{\mu\nu,\mu\nu}^{(N_{\mathrm{BS}})}(k) H^{(N_{\mathrm{BS}})}(k), \tag{20}$$

$$F_{\mu\nu\rho}^{(N_{\mathrm{BS}})}(\mathrm{chair}) = (N_s^3 N_t)^{-1} \prod_{\sigma=1}^{4} \sum_{k_\sigma} \Big[D_{\mu\nu,\mu\nu}^{(N_{\mathrm{BS}})}(k) + D_{\mu\rho,\mu\rho}^{(N_{\mathrm{BS}})}(k) - \frac{1}{2} [(\hat{k}_\mu^{(N_{\mathrm{BS}})})^2 \hat{k}_\nu^{(N_{\mathrm{BS}})} \hat{k}_\rho^{(N_{\mathrm{BS}})} D_{\nu\rho}^{(N_{\mathrm{BS}})}(k) + (\hat{k}_\nu^{(N_{\mathrm{BS}})} \hat{k}_\rho^{(N_{\mathrm{BS}})})^2 D_{\mu\mu}^{(N_{\mathrm{BS}})}(k) - \hat{k}_\mu^{(N_{\mathrm{BS}})} (\hat{k}_\nu^{(N_{\mathrm{BS}})})^2 \hat{k}_\rho^{(N_{\mathrm{BS}})} D_{\mu\rho}^{(N_{\mathrm{BS}})}(k) - \hat{k}_\mu^{(N_{\mathrm{BS}})} \hat{k}_\nu^{(N_{\mathrm{BS}})} (\hat{k}_\rho^{(N_{\mathrm{BS}})})^2 D_{\mu\nu}^{(N_{\mathrm{BS}})}(k)] \Big] \times H^{(N_{\mathrm{BS}})}(k), \tag{21}$$

$$F_{\mu\nu\rho}^{(N_{\mathrm{BS}})}(3\ \mathrm{dim}) = (N_s^3 N_t)^{-1} \prod_{\sigma=1}^{4} \sum_{k_\sigma} \left[\left(1 - \frac{(\hat{k}_\rho^{(N_{\mathrm{BS}})})^2}{4} \right) \times D_{\mu\nu,\mu\nu}^{(N_{\mathrm{BS}})}(k) + \left(1 - \frac{(\hat{k}_\mu^{(N_{\mathrm{BS}})})^2}{4} \right) D_{\nu\rho,\nu\rho}^{(N_{\mathrm{BS}})}(k) + \left(1 - \frac{(\hat{k}_\nu^{(N_{\mathrm{BS}})})^2}{4} \right) D_{\rho\mu,\rho\mu}^{(N_{\mathrm{BS}})}(k) \right] H^{(N_{\mathrm{BS}})}(k), \tag{22}$$

to leading order, where

$$k_\mu^{(N_{\mathrm{BS}})} = 2^{N_{\mathrm{BS}}} k_\mu, \quad \hat{k}_\mu^{(N_{\mathrm{BS}})} = 2 \sin(k_\mu^{(N_{\mathrm{BS}})}/2), \tag{23}$$

$$H^{(N_{\mathrm{BS}})}(k) = \prod_{M=0}^{N_{\mathrm{BS}}-1} \frac{1}{4} \prod_{\mu=1}^{4} [1 + \cos(2^M k_\mu)],$$

TABLE I. Blocked Wilson loops and those in the $N^{\mathrm{BS}} \to \infty$ limit. F_s and F_t are for spatial and space-time Wilson loops, respectively. $N_s^3 \times N_t = 128^3 \times (128\xi)$.

$\xi = 1$ N^{BS}	$F(1\times1)$	$F(1\times2)$	$F(2\times2)$
0	0.500000	0.862251	1.369312
1	0.288104	0.517653	0.879783
2	0.216234	0.403513	0.720860
3	0.194450	0.369800	0.674938
4	0.188403	0.360256	0.660681
∞	0.186476	0.357678	0.658761

$\xi = 2$ N^{BS}	$F_s(1\times1)$	$F_s(1\times2)$	$F_s(2\times1)$	$F_s(2\times2)$
0	0.673095	1.128029	1.128029	1.728563
1	0.402015	0.701155	0.701155	1.145925
2	0.307103	0.555452	0.555452	0.952321
3	0.277085	0.510586	0.510586	0.894124
4	0.268545	0.497689	0.497689	0.876158
∞	0.265709	0.493899	0.493899	0.872921

N^{BS}	$F_t(1\times2)$	$F_t(1\times4)$	$F_t(2\times2)$	$F_t(2\times4)$
0	0.556383	0.920967	0.995852	1.510346
1	0.348216	0.572014	0.655826	1.005403
2	0.274425	0.454023	0.537939	0.837727
3	0.251345	0.418526	0.501772	0.788069
4	0.244845	0.408394	0.491385	0.772639
∞	0.242740	0.405580	0.488471	0.770227

$$D^{(N_{\rm BS})}_{\mu\nu,\mu\nu}(k) = (\hat{k}^{(N_{\rm BS})}_{\mu})^2 D_{\nu\nu}(k) + (\hat{k}^{(N_{\rm BS})}_{\nu})^2 D_{\mu\mu}(k) - 2\hat{k}^{(N_{\rm BS})}_{\mu}\hat{k}^{(N_{\rm BS})}_{\nu}\cos[(2^{N_{\rm BS}-1}-1/2)k_{\mu}] \times \cos[(2^{N_{\rm BS}-1}-1/2)k_{\nu}] D_{\mu\nu}(k). \quad (24)$$

The derivation of Eqs. (20), (21) and (22) is given in the Appendix.

In Table I, we list the numerical results of $F^{(N_{\rm BS})}$ for the case of the standard one plaquette action. We find that the values of $F^{(N_{\rm BS})}$ approach to specific values in the $N_{\rm BS}\to\infty$ limit.

Wilson loops in the limit of infinite $N_{\rm BS}$ can be evaluated as follows. At long distances, the gauge propagator should behave like

$$\langle A^a_{\mu}(x) A^b_{\nu}(0)\rangle = \frac{1}{4\pi^2}\frac{\delta_{\mu\nu}\delta_{a,b}}{x_1^2+x_2^2+x_3^2+x_4^2} + O(1/x^4) \quad (25)$$

in physical unit. In lattice units, it reads

$$\langle A^a_{\mu}(n) A^b_{\nu}(0)\rangle = \delta_{\mu\nu}\delta_{a,b} f_{\mu}(n) + O(1/n^4),$$

$$f_i(n) = \frac{1}{4\pi^2}\frac{1}{n_1^2+n_2^2+n_3^2+\xi^{-2}n_4^2},$$

$$f_4(n) = \frac{1}{4\pi^2}\frac{1}{\xi^2 n_1^2+\xi^2 n_2^2+\xi^2 n_3^2+n_4^2}. \quad (26)$$

The nonleading term of the right-hand side of Eq. (26) does not contribute to the expectation value in the $N_{\rm BS}\to\infty$ limit [20]. Hence we can neglect the higher-order terms. Then the resulting Wilson loops do not depend on the improvement parameters $c_i^{s/t}$ in the original action, since the leading term does not depend on them.

Now, the $(I\times J)$ rectangular Wilson loops in the limit $N_{\rm BS}\to\infty$ are given by

$$F^{(\infty)}_{\mu\nu}(I\times J) = \lim_{N_{\rm BS}\to\infty}\left(\frac{1}{8^{N_{\rm BS}}}\right)^2 \sum_{m,n}\Bigg[2I f_{\mu}(m-n) + 2J f_{\nu}(m-n) + 4\sum_{k=1}^{I-1}(I-k) f_{\mu}(2^{N_{\rm BS}}k\hat{\mu}+m-n) + 4\sum_{k=1}^{J-1}(J-k) f_{\nu}(2^{N_{\rm BS}}k\hat{\nu}+m-n) - 2I f_{\mu}(2^{N_{\rm BS}}J\hat{\nu}+m-n) - 2J f_{\nu}(2^{N_{\rm BS}}I\hat{\mu}+m-n) - 4\sum_{k=1}^{I-1}(I-k) f_{\mu}(2^{N_{\rm BS}}(k\hat{\mu}+J\hat{\nu})+m-n) - 4\sum_{k=1}^{J-1}(J-k) f_{\nu}(2^{N_{\rm BS}}(k\hat{\nu}+I\hat{\mu})+m-n)\Bigg] \quad (27)$$

$$= 2\prod_{\rho=1}^{4}\int_0^1 {\rm d}x_{\rho}(1-x_{\rho})\Bigg[I\tilde{f}_{\mu}(0) + J\tilde{f}_{\nu}(0) + 2\sum_{k=1}^{I-1}(I-k)\tilde{f}_{\mu}(k\hat{\mu}) + 2\sum_{k=1}^{J-1}(J-k)\tilde{f}_{\nu}(k\hat{\nu}) - I\tilde{f}_{\mu}(J\hat{\nu}) - J\tilde{f}_{\nu}(I\hat{\mu}) - 2\sum_{k=1}^{I-1}(I-k)\tilde{f}_{\mu}(k\hat{\mu}+J\hat{\nu}) - 2\sum_{k=1}^{J-1}(J-k)\tilde{f}_{\nu}(k\hat{\nu}+I\hat{\mu})\Bigg], \quad (28)$$

where

$$\tilde{f}_{i=1,2,3}(n) = \frac{1}{4\pi^2}\prod_{\mu=1}^{4}\sum_{\epsilon_{\mu}=\{-1,1\}}\frac{1}{(n_1-\epsilon_1 x_1)^2+(n_2-\epsilon_2 x_2)^2+(n_3-\epsilon_3 x_3)^2+\xi^{-2}(n_4-\epsilon_4 x_4)^2}, \quad (29)$$

$$\tilde{f}_4(n) = \frac{1}{4\pi^2}\prod_{\mu=1}^{4}\sum_{\epsilon_{\mu}=\{-1,1\}}\frac{1}{\xi^2[(n_1-\epsilon_1 x_1)^2+(n_2-\epsilon_2 x_2)^2+(n_3-\epsilon_3 x_3)^2]+(n_4-\epsilon_4 x_4)^2}. \quad (30)$$

Here, we have used $\lim_{N\to\infty}\Sigma_{n=1}^{2^N} f(n/2^N) = \int_0^1 {\rm d}x f(x)$ and a relation $\int_0^1 {\rm d}x\int_0^1 {\rm d}y f(x-y) = \int_0^1 {\rm d}x(1-x)[f(x)+f(-x)]$. Similarly, we obtain

$$F^{(\infty)}_{\mu\nu\rho}({\rm chair}) = 2\prod_{\sigma=1}^{4}\int_0^1 {\rm d}x_{\sigma}(1-x_{\sigma})[\tilde{f}_{\mu}(0)+\tilde{f}_{\nu}(0)+\tilde{f}_{\rho}(0)-\tilde{f}_{\nu}(\hat{\mu})-\tilde{f}_{\rho}(\hat{\mu})-\tilde{f}_{\mu}(\hat{\nu}+\hat{\rho})], \quad (31)$$

$$F^{(\infty)}_{\mu\nu\rho}(3\ {\rm dim}) = 2\prod_{\sigma=1}^{4}\int_0^1 {\rm d}x_{\sigma}(1-x_{\sigma})[\tilde{f}_{\mu}(0)+\tilde{f}_{\nu}(0)+\tilde{f}_{\rho}(0)-\tilde{f}_{\mu}(\hat{\nu}+\hat{\rho})-\tilde{f}_{\nu}(\hat{\rho}+\hat{\mu})-\tilde{f}_{\rho}(\hat{\mu}+\hat{\nu})]. \quad (32)$$

We also denote $F^{(\infty)}$ in Table I.

From the behavior that $F(C)^{(\mathrm{N_{BS}})}$ converges monotonically to $F(C)^{(\infty)}$ which is independent of the coupling parameters $c_i^{s/t}$ in the original action—i.e., the starting point of RG flow—if a block spin transformation is performed from the point at which $F(C)^{(\mathrm{N_{BS}})}$ is already $F(C)^{(\infty)}$, we expect that the value of $F(C)^{(\mathrm{N_{BS}})}$ does not change anymore, which is the property at a fixed point. Therefore we can identify the fixed point by how close the value of $F(C)^{(\mathrm{N_{BS}})}$ is to $F(C)^{(\infty)}$.

Notice that the property of $F(C)^{(\mathrm{N_{BS}})}$ also suggests that an RG flow from every point in the critical surface flows into one RG flow (RT) in finite β, on which $F(C)^{(\mathrm{N_{BS}})}$ is $F(C)^{(\infty)}$, as shown in Fig. 1, since the starting point $c_i^{s/t}$ of the infinite block spin transformations for $F(C)^{(\infty)}$ must be in $\beta=\infty$ $(g=0)$.

V. ANISOTROPIC RG-IMPROVED ACTION

We search for an action which reproduces the values of Wilson loops in the $N_{\mathrm{BS}}\to\infty$ limit as much as possible within the restricted coupling parameter space of the action, Eq. (2). For this purpose, Iwasaki considered the average relative deviation of Wilson loops,

$$R^{(N_{\mathrm{BS}})}=\sqrt{\sum_C\left(\frac{F^{(N_{\mathrm{BS}})}(C)-F^{(\infty)}(C)}{F^{(\infty)}(C)}\right)^2 w(C)}, \quad (33)$$

where Σ_C is over four-loop shapes up to length 6—plaquette (10), 1×2 rectangular loop (11), chair (12), and three-dimensional loop (13)—with a uniform weight $w(C)=1/4$. Equation (33) means that, when $R^{(N_{\mathrm{BS}})}=0.01$, for example, the deviation of small Wilson loops from their values in the $N_{\mathrm{BS}}\to\infty$ limit is about 1% after N_{BS} block spin transformations.

On anisotropic lattices, we generalize Eq. (33) by subdividing each loop shape into orientations and adopt a uniform weight for each orientation. Namely, because we have three spatial and three temporal plaquette orientations, we give $w(\text{spatial plaquette})=w(\text{temporal plaquette})=1/8$. For 1×2 rectangular loops, we have six orientations of spatial loops, three orientations of $W_{k4}^{(2\times1)}$, and three orientations of $W_{k4}^{(1\times2)}$. Therefore, we give 1/8, 1/16, and 1/16 for their weights. Similarly, we subdivide 12 chair and 4 three-dimensional loop orientations.

Here, we should emphasize that we are trying to reproduce the values of $F^{(\infty)}(C)$ for ten different Wilson loops by controlling three coupling parameters for $\xi\neq1$ (four Wilson loops by one parameter for $\xi=1$) at the same time, which is a quite nontrivial trial, and the value of $R^{(N_{\mathrm{BS}})}$ indicates that $F^{(N_{\mathrm{BS}})}(C)$ does not change within the accuracy of $R^{(N_{\mathrm{BS}})}$ under block spin transformations, since $F^{(N_{\mathrm{BS}})}(C)$ approaches to $F^{(\infty)}(C)$ as N_{BS} increases and the change of $F^{(N_{\mathrm{BS}})}(C)$ is smaller than the difference. Therefore, by measuring the indicator $R^{(N_{\mathrm{BS}})}$, we can check indirectly how ''slowly'' the coupling parameters flow—i.e., how the nearest point which we find in the restricted parameter space is close to the real fixed point in the weak coupling limit.

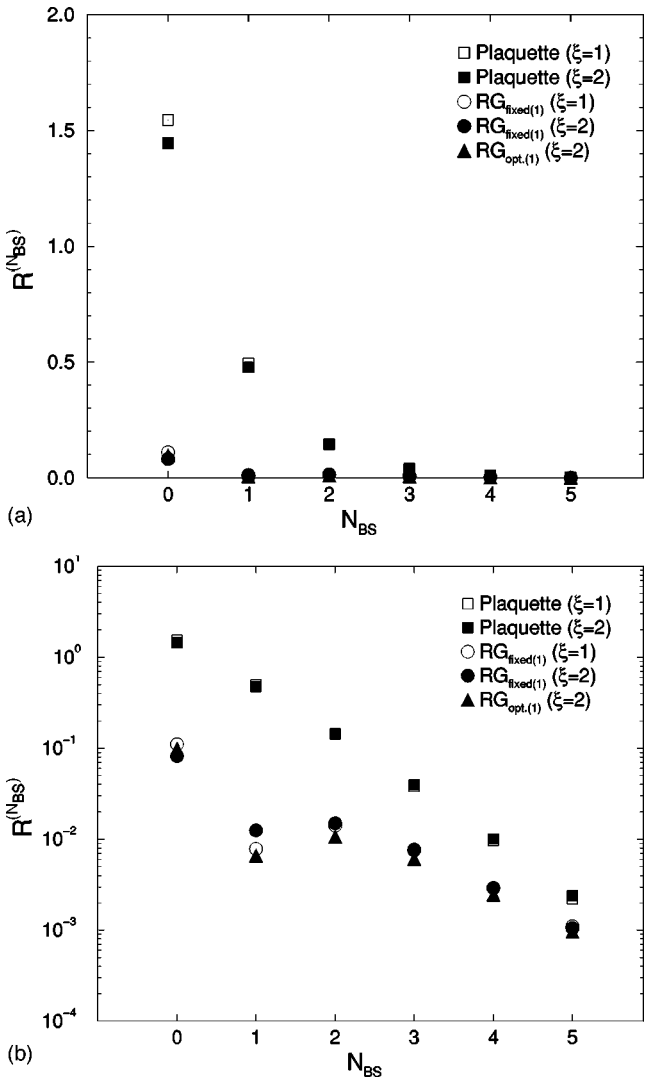

FIG. 2. $R^{(N_{\mathrm{BS}})}$ vs N_{BS} at $\xi=1$ and 2 for various actions. Open symbols are for $\xi=1$ and solid symbols are for $\xi=2$. Results from the standard one-plaquette action are shown by squares. $\mathrm{RG_{opt}}(n)$ is the RG-improved action which minimizes $R^{(n)}$ on the lattice with the anisotropy ξ. $\mathrm{RG_{fixed}}(n)$ is an approximate RG-improved action using the values of $c_i^{s/t}$ for $\xi=1$.

In Fig. 2, we show the N_{BS} dependence of $R^{(N_{\mathrm{BS}})}$ for $\xi=1$ and 2. The results from the plaquette action (open and solid squares) show exponential decrease with N_{BS}. (Results from RG-improved actions will be discussed later.)

We search for the minimum point of $R^{(N_{\mathrm{BS}})}$ in the parameter space (c_1^s,c_1^t,c_2^t) for each value of ξ. Figure 3 shows the behavior of $R^{(1)}$ for $\xi=2$ in the subspaces $c_1^t=c_2^t$ and $c_1^s=-0.31$. Figure 3(b) suggests that the region of small $R^{(N_{\mathrm{BS}})}$ spreads in the direction of constant $c_1^t+c_2^t$, which we confirm also for other cases.

To find the minimum of $R^{(N_{\mathrm{BS}})}$, we solve the equations

$$\frac{\partial(R^{(N_{\mathrm{BS}})})^2}{\partial c_i}=\sum_C 2\frac{\partial F^{(N_{\mathrm{BS}})}(C)}{\partial c_i}\frac{F^{(N_{\mathrm{BS}})}(C)-F^{(\infty)}(C)}{[F^{(\infty)}(C)]^2}w(C)=0, \quad (34)$$

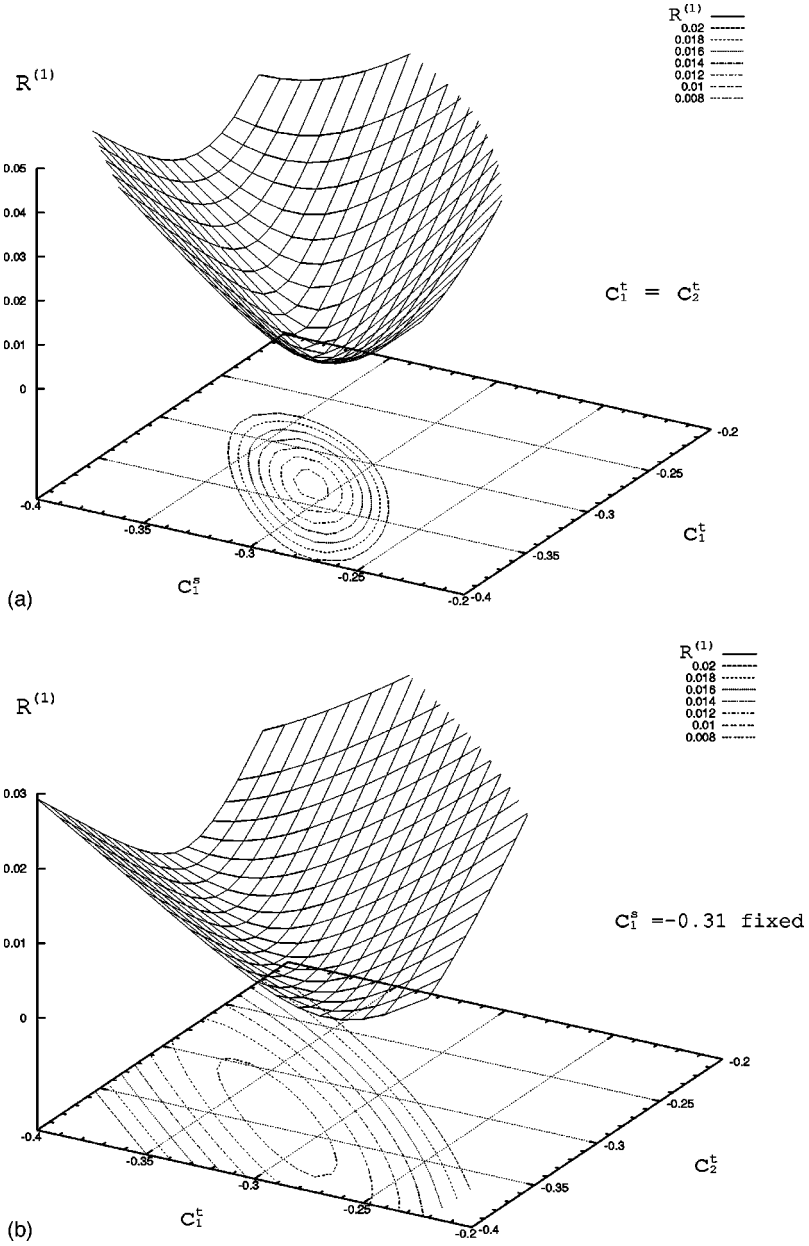

FIG. 3. $R^{(1)}$ for $\xi=2$ (a) in the subspace $c_1^t=c_2^t$ as a function of $(c_1^s,c_1^t=c_2^t)$, (b) in the subspace $c_1^s=-0.31$ as a function of (c_1^t,c_2^t).

with $c_i=\{c_1^s,c_1^t,\ c_2^t\}$. We iteratively solve Eq. (34) using linear approximations

$$\sum_C \left(\left. \frac{\partial F^{(N_{\rm BS})}(C)}{\partial c_i} \right|_{(c_{10}^s,c_{10}^t,c_{20}^t)} \right)^2 \frac{w(C)}{[F^{(\infty)}(C)]^2}(c_i-c_{i0}) = \sum_C \left. \frac{\partial F^{(N_{\rm BS})}(C)}{\partial c_i} \right|_{(c_{10}^s,c_{10}^t,c_{20}^t)} \times \frac{F^{(\infty)}(C)-F^{(N_{\rm BS})}(C)|_{(c_{10}^s,c_{10}^t,c_{20}^t)}}{[F^{(\infty)}(C)]^2} w(C), \qquad (35)$$

around $(c_{10}^s,c_{10}^t,c_{20}^t)$, where $\partial F^{(N_{\rm BS})}(C)/\partial c_i$ can be calculated by

$$\frac{\partial D_{\mu\nu}}{\partial c_i} = -D_{\mu\nu}\frac{\partial D_{\mu\nu}^{-1}}{\partial c_i} D_{\mu\nu}, \qquad (36)$$

with $D_{\mu\nu}^{-1}$ given by Eq. (8). We solve the equations numerically on a 128^4 lattice. We checked that the finite volume effects are sufficiently small for the Wilson loops in Eq. (33).

Results for the improvement parameters which minimize $R^{(N_{\rm BS})}$ are summarized in Table II and Figs. 4 and 5 for $N_{\rm BS}=1$ and 2. We also show the results for $N_{\rm BS}=0$ in Fig. 6. In these figures, c_1^s, c_1^t, and c_2^t are shown by solid, dashed, and dot-dashed lines. In the followings we denote the corresponding action as $\mathrm{RG}_{\mathrm{opt}(N_{\rm BS})}$ [the RG-improved action with the ξ-dependent optimum values of (c_1^s,c_1^t,c_2^t) to minimize $R^{(N_{\rm BS})}$]. At $\xi=1$, we reproduce Iwasaki's results [20] $c_1^s=c_i^t=c_2^t=-0.331$ (-0.293) for $N_{\rm BS}=1(2)$.

Figure 7 shows the values of $R^{(N_{\rm BS})}$ from $\mathrm{RG}_{\mathrm{opt}(N_{\rm BS})}$ for

TABLE II. The improvement parameters (c_1^s, c_1^t, c_2^t) and $R^{(N_{\rm BS})}$ of the RG-improved action $\mathrm{RG}_{\mathrm{opt}(N_{\rm BS})}$ for $N_{\rm BS}=1$ and 2 at various ξ.

$N_{\rm BS}$	ξ	c_1^s	c_1^t	c_2^t	$R^{(N_{\rm BS})}$
1	0.20	−0.349	−0.359	−0.073	5.40×10^{-3}
1	0.25	−0.357	−0.356	−0.097	5.33×10^{-3}
1	0.50	−0.363	−0.345	−0.204	6.10×10^{-3}
1	0.70	−0.350	−0.338	−0.271	7.14×10^{-3}
1	0.90	−0.337	−0.333	−0.316	7.67×10^{-3}
1	1.00	−0.331	−0.331	−0.331	7.73×10^{-3}
1	1.10	−0.326	−0.329	−0.341	7.68×10^{-3}
1	1.50	−0.313	−0.324	−0.356	7.07×10^{-3}
1	2.00	−0.307	−0.316	−0.350	6.52×10^{-3}
1	2.50	−0.307	−0.302	−0.340	6.58×10^{-3}
1	3.00	−0.308	−0.286	−0.331	6.96×10^{-3}
1	3.50	−0.311	−0.270	−0.325	7.39×10^{-3}
1	4.00	−0.314	−0.255	−0.320	7.77×10^{-3}
1	4.50	−0.317	−0.241	−0.316	8.07×10^{-3}
1	5.00	−0.320	−0.229	−0.312	8.30×10^{-3}
1	6.00	−0.327	−0.208	−0.306	8.59×10^{-3}
1	7.00	−0.333	−0.192	−0.302	8.73×10^{-3}
1	8.00	−0.339	−0.178	−0.298	8.77×10^{-3}
2	0.20	−0.360	−0.282	−0.122	1.34×10^{-3}
2	0.25	−0.358	−0.282	−0.142	1.37×10^{-3}
2	0.50	−0.328	−0.284	−0.225	1.87×10^{-3}
2	0.70	−0.309	−0.287	−0.265	2.25×10^{-3}
2	0.90	−0.297	−0.291	−0.287	2.42×10^{-3}
2	1.00	−0.293	−0.293	−0.293	2.43×10^{-3}
2	1.10	−0.290	−0.294	−0.297	2.42×10^{-3}
2	1.50	−0.284	−0.299	−0.303	2.20×10^{-3}
2	2.00	−0.283	−0.299	−0.304	1.91×10^{-3}
2	2.50	−0.284	−0.295	−0.303	1.82×10^{-3}
2	3.00	−0.287	−0.287	−0.304	1.91×10^{-3}
2	3.50	−0.290	−0.277	−0.305	2.09×10^{-3}
2	4.00	−0.294	−0.268	−0.306	2.30×10^{-3}
2	4.50	−0.298	−0.258	−0.308	2.50×10^{-3}
2	5.00	−0.302	−0.249	−0.309	2.68×10^{-3}
2	6.00	−0.311	−0.232	−0.310	2.98×10^{-3}
2	7.00	−0.320	−0.218	−0.310	3.20×10^{-3}
2	8.00	−0.330	−0.205	−0.309	3.36×10^{-3}

$N_{\rm BS}=0$, 1, and 2 [dashed (short), dashed (long), and dot-dashed lines, respectively]. We find that the values of $R^{(N_{\rm BS})}$ remain small in a wide range of ξ, indicating that a similar quality of improvement is achieved by the program of RG improvement even at $\xi\neq1$.

Here, it is worth noting that reducing the number of independent coupling parameters has a practical benefit in numerical simulations. In particular, because a nontrivial ξ dependence in coupling parameters makes the calculation of thermodynamic quantities complicated, it is attractive to adopt ξ-independent improvement parameters.

Therefore, we study $R^{(N_{\rm BS})}$ at $\xi\neq1$ with the improved parameters fixed to the optimum value at $\xi=1$, $c_1^s=c_1^t=c_2^t(=-0.331$ for $N_{\rm BS}=1)$. We denote this action as $\mathrm{RG}_{\mathrm{fixed}(N_{\rm BS})}$ (an RG-improved action with c_1^s, c_1^t, and c_2^t fixed to the Iwasaki's value minimizing $R^{(N_{\rm BS})}$ on the $\xi=1$ lattice). The result of $R^{(1)}$ for $N_{\rm BS}=1$ is plotted by the solid line in Fig. 7. We also study the case $c_1^s=c_1^t=c_2^t\equiv c_1(\xi)$ where c_1 is varied to minimize $R^{(N_{\rm BS})}$ at each ξ. The results for the minimum value of $R^{(1)}$ and the corresponding optimum value of the parameter c_1 are shown by dotted lines in Figs. 7 and 4, respectively. For both cases, $R^{(1)}$ becomes larger as ξ deviates from 1. It means that one cannot keep the same quality of improvement in the whole range of ξ with the $\mathrm{RG}_{\mathrm{fixed}(N_{\rm BS})}$ action or the action with the constraint $c_1^s=c_1^t=c_2^t=c_1(\xi)$.

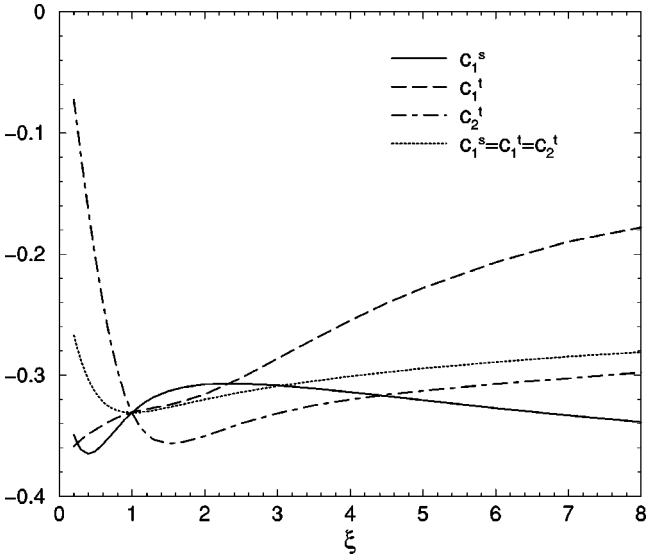

FIG. 4. Improvement parameters (c_1^s, c_1^t, c_2^t) for the RG-improved action $\mathrm{RG}_{\mathrm{opt}(1)}$ which minimizes $R^{(1)}$ at each ξ. The dotted line is the solution which minimizes $R^{(1)}$ when a constraint $c_1^s=c_1^t=c_2^t$ is required.

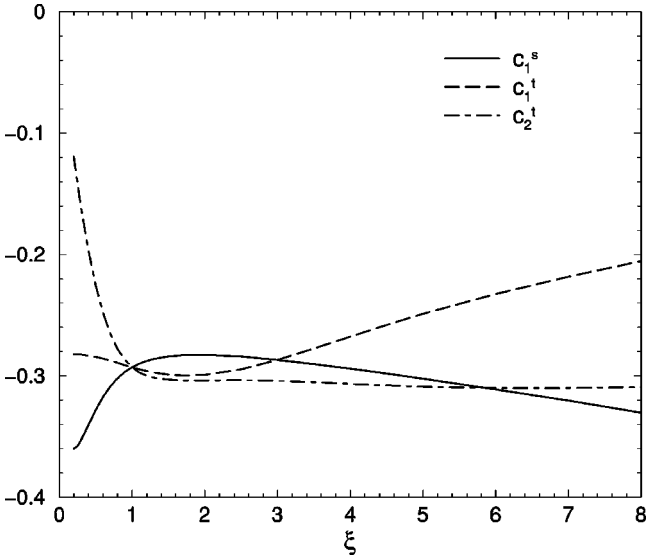

FIG. 5. Improvement parameters (c_1^s, c_1^t, c_2^t) for the RG-improved action $\mathrm{RG}_{\mathrm{opt}(2)}$ which minimizes $R^{(2)}$ at each ξ.

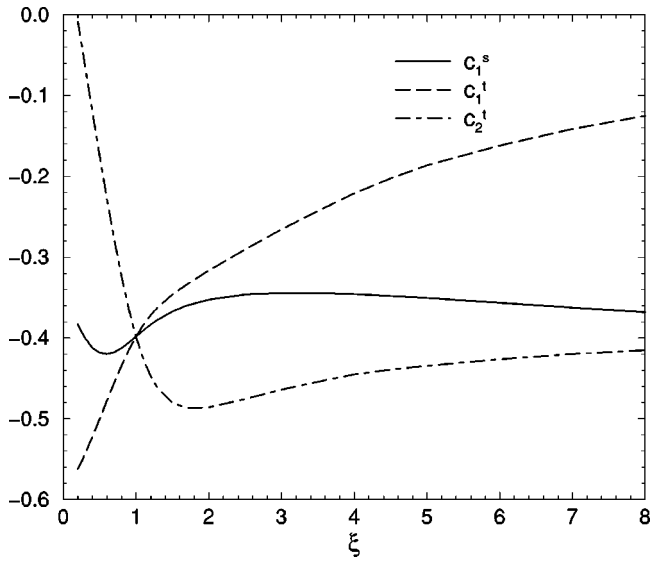

FIG. 6. The same as Fig. 5, but for the $RG_{opt(0)}$ which minimizes $R^{(0)}$.

In most simulations, however, we are interested in the cases of $\xi \approx 1-4$, where the values of $R^{(1)}$ remain $O(10^{-2})$. In the determination of an RG-improved action, the difference between Fig. 4 for $N_{BS}=1$ and Fig. 5 for $N_{BS}=2$ is a matter of taste: Both actions are equally qualified with $R^{(N_{BS})} \leqslant O(10^{-2})$ and the difference in the values of improvement parameters should be regarded as a freedom in the choice. In this respect, we find that the variations of improvement parameters as functions of ξ are small for $\xi \approx 1-4$.

In Fig. 8, we show $R^{(1)}$ for various actions including the standard plaquette action and the Symanzik improved actions. For RG-improved actions, results are shown for $RG_{opt(1)}$ and $RG_{fixed(1)}$. Similar results are obtained for other

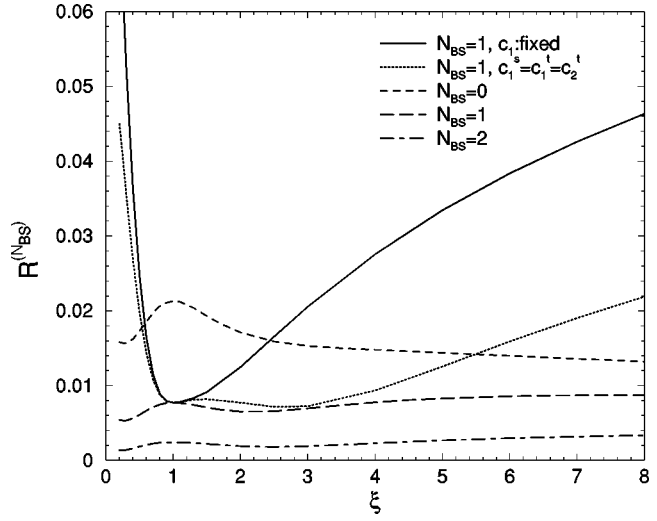

FIG. 7. $R^{(N_{BS})}$ as functions of ξ from the RG-improved actions $RG_{opt(N_{BS})}$ for $N_{BS}=0$, 1 and 2. Also plotted are the results for $R^{(1)}$ determined from $RG_{fixed(1)}$ (solid line), and the minimum $R^{(1)}$ obtained with the constraint $c_1^s=c_1^t=c_2^t$ (dotted line).

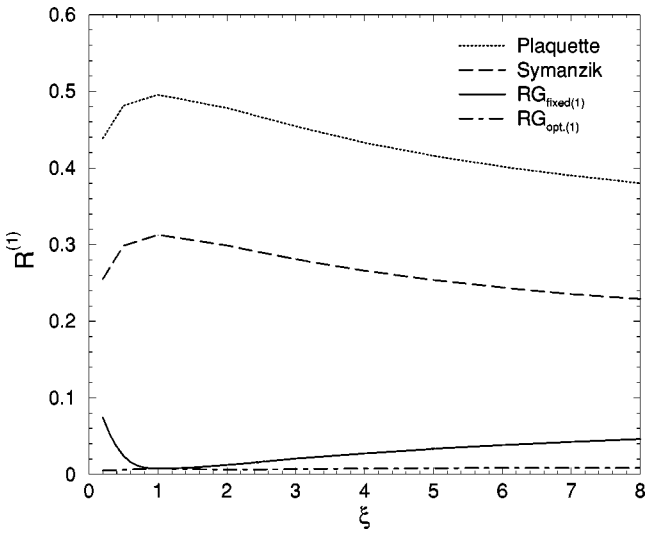

FIG. 8. $R^{(1)}$ for various actions as functions of ξ.

values of N_{BS}, too. We find that, although a stable improvement is achieved with the $RG_{opt(1)}$ action for a wide range of ξ, when we restrict ourselves to the range $\xi \approx 1-4$, all RG-improved actions lead to quite small values of $R^{(1)} \lesssim O(10^{-2})$; i.e., the average deviation of small Wilson loops from the $N_{BS}=\infty$ limit is less than about 1% after one blocking. On the other hand, for the standard plaquette and Symanzik actions, typical values of $R^{(1)}$ are 0.4–0.5 and 0.25–0.3, respectively. We conclude that the $RG_{fixed(N_{BS})}$ action, in which the improvement parameters are fixed to Iwasaki's value for $\xi=1$, improves the theory well at $\xi \approx 1-4$.

VI. CONCLUSIONS

We studied RG-improved actions for the SU(3) gauge theory on anisotropic lattices, following Iwasaki's program of improvement. We determined the improvement parameters as functions of the anisotropy ξ for the action with plaquette and 1×2 rectangular terms. We found that the program of improvement works well even on anisotropic lattices without losing the quality of improvement if we adjust three improvement parameters (c_1^s, c_1^t, c_2^t) as functions of ξ.

Moreover, we discussed a practical choice of improved action for numerical simulations on anisotropic lattices. From a calculation of an indicator which estimates the distance to the renormalized trajectory near the fixed point, we found that keeping the improvement parameters to the values at $\xi=1$ leads to the distance comparable to the minimum distance at the optimum (c_1^s, c_1^t, c_2^t), for the range of the anisotropy $\xi \approx 1-4$. This means that, for the range $\xi \approx 1-4$ where anisotropic lattices are expected to be efficient in calculating thermodynamic quantities [10], the choice of Iwasaki's value for improvement parameters is acceptable also for $\xi \neq 1$, as adopted in a previous work [11].

As the next step, it is necessary to confirm whether good properties of the RG-improved action at $\xi=1$ maintain also at $\xi \neq 1$ in practical simulations, but we showed that the Iwasaki's program of an RG-improved action can be generalized for $\xi \neq 1$.

ACKNOWLEDGMENTS

We thank the members of the CP-PACS Collaboration and S. Hands for helpful comments and discussions. This work is supported in part by Grants-in-Aid of the Ministry of Education, Culture, Sports, Science and Technology, Japan (No. 13640260). S.E. is supported by PPARC grant PPA/G/S/1999/00026. T.U. is supported by the public research organizations at Center for Computational Physics (CCP), University of Tsukuba.

APPENDIX: DERIVATION OF THE WILSON LOOP AFTER BLOCK SPIN TRANSFORMATION

We derive Eqs. (20), (21), and (22) following Appendix B of Ref. [20]. Let us introduce the Fourier transformation

$$A_\mu^{(N_{\rm BS})}(x)=\int_k \mathrm{e}^{i2^{N_{\rm BS}}(kx+k_\mu/2)}\tilde{A}_\mu^{(N_{\rm BS})}(k), \tag{A1}$$

where the lattice spacing for $A_\mu^{(N_{\rm BS})}(x)$ is $2^{N_{\rm BS}}a$. From Eqs. (4), (18), and (A1), we obtain

$$\tilde{A}_\mu^{(N_{\rm BS})}(k)=\mathrm{e}^{-i(2^{N_{\rm BS}-1}-1/2)k_\mu}\tilde{H}^{(N_{\rm BS})}(k)\tilde{A}_\mu^{(0)}(k), \tag{A2}$$

where

$$\tilde{H}^{(N_{\rm BS})}(k)=\prod_{M=0}^{N_{\rm BS}-1}\frac{1}{8}\prod_{\nu=1}^{4}(\mathrm{e}^{i2^M k_\nu}+1). \tag{A3}$$

We define the free propagator $D_{\mu\nu}^{(N_{\rm BS})}$ for the field $\tilde{A}^{(N_{\rm BS})}$ by

$$\langle\tilde{A}_\mu^{a(N_{\rm BS})}(k)\tilde{A}_\nu^{b(N_{\rm BS})}(k')\rangle=\delta_{a,b}\delta(k+k')D_{\mu\nu}^{(N_{\rm BS})}(k). \tag{A4}$$

We obtain

$$D_{\mu\nu}^{(N_{\rm BS})}(k)=\mathrm{e}^{-i(2^{N_{\rm BS}-1}-1/2)k_\mu}\mathrm{e}^{i(2^{N_{\rm BS}-1}-1/2)k_\nu}H^{(N_{\rm BS})}(k)D_{\mu\nu}(k), \tag{A5}$$

where $H^{(N_{\rm BS})}(k)$ is given by Eq. (24).

The expectation value of Wilson loops that can be written as

$$W(C)=\sum_{\mu,\nu}c_{\mu\nu}(k)D_{\mu\nu}(k) \tag{A6}$$

for the original lattice is obtained for the $N_{\rm BS}$th blocked lattice by

$$W^{(N_{\rm BS})}(C)=\sum_{\mu,\nu}c_{\mu\nu}(2^{N_{\rm BS}}k)D_{\mu\nu}^{(N_{\rm BS})}(k). \tag{A7}$$

To derive Eq. (24), we used the fact that $D_{\mu\nu}(k)$ is odd in k_μ and k_ν when $\mu\neq\nu$.

[1] CP-PACS Collaboration, A. Ali Khan *et al.*, Phys. Rev. D **65**, 054505 (2002); CP-PACS Collaboration, A. Ali Khan *et al.*, Phys. Rev. Lett. **85**, 4674 (2000).

[2] CP-PACS Collaboration, S. Aoki *et al.*, Phys. Rev. D **60**, 114508 (1999).

[3] Y. Iwasaki, K. Kanaya, S. Kaya, and T. Yoshié, Phys. Rev. Lett. **78**, 179 (1997).

[4] CP-PACS Collaboration, A. Ali Khan *et al.*, Phys. Rev. D **63**, 034502 (2000).

[5] C. Bernard *et al.*, Phys. Rev. D **58**, 014503 (1998); Nucl. Phys. B (Proc. Suppl.) **106**, 412 (2002).

[6] U.M. Heller, F. Karsch, and B. Sturm, Phys. Rev. D **60**, 114502 (1999); F. Karsch, E. Laermann, and A. Peikert, Phys. Lett. B **478**, 447 (2000); Nucl. Phys. **B605**, 579 (2001).

[7] C. Bernard *et al.*, Phys. Rev. D **55**, 6861 (1997).

[8] CP-PACS Collaboration, A. Ali Khan *et al.*, Phys. Rev. D **64**, 074510 (2001).

[9] S. Ejiri, Nucl. Phys. B (Proc. Suppl.) **94**, 19 (2001).

[10] CP-PACS Collaboration, Y. Namekawa *et al.*, Phys. Rev. D **64**, 074507 (2001).

[11] S. Sakai, A. Nakamura, and T. Saito, Nucl. Phys. **A638**, 535 (1998); S. Sakai, T. Saito, and A. Nakamura, Nucl. Phys. **B584**, 528 (2000).

[12] QCD-TARO Collaboration, Ph. de Forcrand *et al.*, Phys. Rev. D **63**, 054501 (2001).

[13] T. Umeda, R. Katayama, O. Miyamura, and H. Matsufuru, Nucl. Phys. B (Proc. Suppl.) **94**, 435 (2001); Int. J. Mod. Phys. A **61**, 2215 (2001)

[14] T.R. Klassen, Nucl. Phys. B (Proc. Suppl.) **73**, 918 (1999); P. Chen, Phys. Rev. D **64**, 034509 (2001).

[15] G.S. Bali and P. Boyle, Phys. Rev. D **59**, 114504 (1999); G.S. Bali, *ibid.* **62**, 114503 (2000).

[16] CP-PACS Collaboration, M. Okamoto *et al.*, Phys. Rev. D **65**, 094508 (2002).

[17] CP-PACS Collaboration, T. Manke *et al.*, Phys. Rev. Lett. **82**, 4396 (1999).

[18] C.J. Morningstar and M. Peardon, Phys. Rev. D **56**, 4043 (1997); **60**, 034509 (1999).

[19] C. Liu, J. Zhang, Y. Chen, and J.P. Ma, Nucl. Phys. **B624**, 360 (2002).

[20] Y. Iwasaki, Nucl. Phys. **B258**, 141 (1985); University of Tsukuba Report No. UTHEP-118, 1983.

[21] F. Karsch, Nucl. Phys. **B205**, 285 (1982).

[22] G. Burgers, F. Karsch, A. Nakamura, and I.O. Stamaescu, Nucl. Phys. **B304**, 587 (1988).

[23] T.R. Klassen, Nucl. Phys. **B533**, 557 (1998).

[24] S. Ejiri, Y. Iwasaki, and K. Kanaya, Phys. Rev. D **58**, 094505 (1988).

[25] J. Engels, F. Karsch, and T. Scheideler, Nucl. Phys. **B564**, 303 (2000).

[26] M. Alford, T.R. Klassen, and G.P. Lepage, Phys. Rev. D **58**, 034503 (1998).

[27] C. Morningstar, Nucl. Phys. B (Proc. Suppl.) **53**, 914 (1997).

[28] M. Alford, I.T. Drummond, R.R. Horgan, H. Shanahan, and M. Peardon, Phys. Rev. D **63**, 074501 (2001).
[29] P. Harsenfratz and F. Niedermayer, Nucl. Phys. **B414**, 785 (1994).
[30] QCD-TARO Collaboration, P. de Forcrand *et al.*, Nucl. Phys. **B577**, 263 (2000).
[31] P. Rüefenacht and U. Wenger, Nucl. Phys. **B616**, 163 (2001).
[32] Y. Iwasaki, K. Kanaya, T. Kaneko, and T. Yoshié, Phys. Rev. D **56**, 151 (1997).
[33] CP-PACS Collaboration, A. Ali Khan *et al.*, Phys. Rev. D **63**, 114504 (2001); **64**, 114506 (2001); CP-PACS Collaboration, J.-I. Noaki *et al.*, *ibid.* (to be published), hep-lat/0108013.
[34] C. Morningstar and M. Peardon, Nucl. Phys. B (Proc. Suppl.) **47**, 258 (1996).
[35] P. Weisz, Nucl. Phys. **B212**, 1 (1983).